International Urology and Nephrology (2019) 51:817–824
https://doi.org/10.1007/s11255-019-02134-0

UROLOGY - ORIGINAL PAPER

The clinical utility of prostate cancer heterogeneity using texture analysis of multiparametric MRI

Maira Hameed[1] · Balaji Ganeshan[2] · Joshua Shur[3] · Subhabrata Mukherjee[4] · Asim Afaq[2] · Deepak Batura[5]

Received: 16 February 2019 / Accepted: 21 March 2019 / Published online: 30 March 2019
© Springer Nature B.V. 2019

Abstract

Purpose To determine if multiparametric MRI (mpMRI) derived filtration-histogram based texture analysis (TA) can differentiate between different Gleason scores (GS) and the D'Amico risk in prostate cancer.

Methods We retrospectively studied patients whose pre-operative 1.5T mpMRI had shown a visible tumour and who subsequently underwent radical prostatectomy (RP). Guided by tumour location from the histopathology report, we drew a region of interest around the dominant visible lesion on a single axial slice on the *T*2, Apparent Diffusion Coefficient (ADC) map and early arterial phase post-contrast *T*1 image. We then performed TA with a filtration-histogram software (TexRAD -Feedback Medical Ltd, Cambridge, UK). We correlated GS and D'Amico risk with texture using the Spearman's rank correlation test.

Results We had 26 RP patients with an MR-visible tumour. Mean of positive pixels (MPP) on ADC showed a significant negative correlation with GS at coarse texture scales. MPP showed a significant negative correlation with GS without filtration and with medium filtration. MRI contrast texture without filtration showed a significant, negative correlation with D'Amico score. MR *T*2 texture showed a significant, negative correlation with the D'Amico risk, particularly at textures without filtration, medium texture scales and coarse texture scales.

Conclusion ADC map mpMRI TA correlated negatively with GS, and *T*2 and post-contrast images with the D'Amico risk score. These associations may allow for better assessment of disease prognosis and a non-invasive method of follow-up for patients on surveillance. Further, identifying clinically significant prostate cancer is essential to reduce harm from over-diagnosis and over-treatment.

Keywords Prostatic neoplasms · Radical prostatectomy · Neoplasm grading · Prostate-specific antigen · Magnetic resonance imaging · Image enhancement · Texture analysis

Introduction

The histological Gleason score (GS) is an essential determinant for the management of prostate cancer. The D'Amico risk stratification score is another frequently used tool, which uses a combination of clinical and imaging data with histology to gauge the 5-year risk of treatment failure [1]. Risk stratification in this way helps select patients suitable for active treatment and avoids over-treatment of clinically insignificant disease [2–4]. Current risk stratification is limited to clinical examination, serum prostate-specific antigen, and transrectal prostate biopsy.

Multi-parametric MRI (mpMRI) has revolutionised the detection, staging, and management of early prostate cancer and now plays a central role [5–8]. mpMRI provides anatomical as well as at least two functional sequences, and includes *T*1- and *T*2-weighted, dynamic

✉ Deepak Batura
deepakbatura@gmail.com

1 Department of Radiology, Imperial College Healthcare NHS Trust, South Wharf Road, London, UK

2 Institute of Nuclear Medicine, University College London Hospitals NHS Foundation Trust, Euston Road, London, UK

3 Joint Department of Medical Imaging, University Health Network, Toronto, Canada

4 Department of Urology, Dartford and Gravesham NHS Trust, Darenth Wood Road, Dartford, UK

5 Department of Urology, London North West University Healthcare NHS Trust, Watford Road, London, UK

contrast-enhanced, and diffusion weighting imaging [9]. This imaging modality provides a vast amount of data which may be useful. In particular, there has been a surge of work regarding texture analysis in a variety of malignancies including prostate cancer [10–15].

Tumour heterogeneity is a crucial factor in predicting a tumour's malignant potential at a cellular level. Texture analysis (TA) provides a means to quantify signal heterogeneity in images through analysis of the regularity and coarseness of pixel value spatial distribution not visually perceptible to the human eye [16]. The filtration-histogram technique of TA is one of the methods commonly employed and validated to derive quantitative textural features [17]. The revised Pi-RADS 2 guidelines now advocate the use of tumour signal homogeneity on mpMRI to grade disease [9]. In the patient subset where a tumour is not visible, the additional data provided by quantitative TA (QTA) may have utility in detecting clinically significant disease. Histogram analysis with/without an initial filtration step is a commonly employed technique in the field of TA [11–20].

This study aimed to evaluate the use of filtration-histogram TA derived from mpMRI to differentiate the Gleason score of prostatic tumour. A secondary outcome measure was the correlation between MR texture analysis and the D'Amico risk category as well as the total serum PSA.

Methods

According to the Health Research Authority, UK, recommendations [21], local institutional review board approval was not sought for this retrospective review of anonymised, routinely acquired patient clinical and imaging data.

Patients

The study population was men with prostate adenocarcinoma who underwent mpMRI followed by prostatectomy from June 2013 to September 2016. Men who did not have surgery or pre-operative MRI were excluded, as were men who did not have a visible tumour focus on imaging. In total, the study included 26 men with mean age 64.7 ± 6.4 (48, 74) years, of which 13/26 = 50% had a Gleason score of 3 + 4 or less (ISUP grade group 1 and 2), and 13/26 = 50% had a Gleason's score of 4 + 3 or greater (ISUP grade group 3 or more), Table 1.

We calculated the D'Amico risk score from the biopsy GS, PSA value closest to the date of diagnosis and clinical stage. Details of the D'Amico risk classification is in Table 2 [1].

Table 1 Demographic data of study population

	Mean ± (SD) (range), median
Age	64.7 ± 6.4 (48, 74), 66
PSA (ng/ml)	8.7 ± 5.2 (1.6, 23), 7.9
Prostate volume (cc)	37 ± 13.3 (15, 70), 34.5
PSA density (ng/ml/cc)	0.3 ± 0.2 (0.05, 0.79), 0.2
Tumour volume (ml)	2.6 ± 2.3 (0.99, 11), 1.98
Path stage	*n* (%)
*T*2a	2 (7.7)
*T*2b	1 (3.8)
*T*2c	9 (34.6)
*T*3a	7 (26.9)
*T*3b	6 (23.1)
*T*3c	0
*T*4	1 (3.8)
Gleason	*n* (%)
3 + 3	1 (3.8)
3 + 4	12 (46.2)
4 + 3	9 (34.6)
4 + 4	0
4 + 5	3 (11.5)
5 + 4	1 (3.8)
D'Amico	*n* (%)
Intermediate	13 (50)
High	13 (50)

PSA prostate-specific antigen

Table 2 D'Amico risk classification

Low-risk	GS ≤ 6 and PSA ≤ 10 ng/ml and clinical stage *T*1c or *T*2
Intermediate risk	GS = 7 or PSA > 10 and ≤ 20 ng/ml or clinical stage *T*2b
High risk	GS ≥ 8 or PSA ≥ 20 ng/ml or clinical stage *T*2c 0r *T*3

GS highest biopsy Gleason score, *PSA* prostate-specific antigen

MRI

MpMRI of the prostate gland was performed with a 1.5T MRI scanner (Aera, Siemens Healthcare, Erlangen, Germany). The MRI protocol included axial small field-of-view *T*2 weighted; axial diffusion-weighted imaging (DWI) and dynamic post-contrast sequences (DWI) following administration of 20 mg of Hyoscine Butylbromide (Buscopan, Boehringer Ingelheim, Ingelheim, Germany). MpMRI acquisition parameters are in Table 3.

Table 3 MRI acquisition parameters

Sequence	TR (ms)	TE (ms)	NA	BR	ST (mm)	PAT	Fat suppression	Receiver bandwidth (Hz/pixel)
*T*2 Blade	5500	100	1	320	3	2	None	382
DWI b0, 500, 1000, 1400	6800	99	5	160	3.5	2	SPAIR	1250
*T*1 3D VIBE axial dynamic	6.91	1.71	1	256	3	2	SPAIR	300

TR repetition time, *TE* echo time, *NA* number of averages, *BR* base resolution, *ST* slice thickness, *PAT* parallel acquisition technique, *SPAIR* spectral attenuated inversion recovery, *VIBE* volumetric interpolated breath-hold examination

Histopathology

A histopathologist specialising in prostate cancer reported all prostatectomy specimens. Gleason grade and ISUP grade groups were evaluated with patients scored as clinically significant (4+3 or higher) or clinically not significant (3+4 or less) [22].

Histology-MRI matching

Following identification of MRI-visible tumour matched to the histopathology report, the tumour focus was contoured on the single axial image containing the largest visible tumour diameter to form a region of interest (ROI) on the *T*2, ADC and early post-contrast sequences.

Texture analysis

MR texture analysis (MRTA) was performed on the ROIs using commercially available TA research software (TexRAD, Feedback Medical Ltd, Cambridge, UK—www.fbkmed.com). MRTA comprised a filtration-histogram technique which has been described previously [17, 19]. In brief, filtration step extracted and enhanced features of different signal intensity and sizes corresponding to a spatial scale filter (SSF) which varied from 0 (without filtration), 2 mm (fine texture scale), 3–5 mm (medium texture scale) and 6 mm (coarse texture scale). An illustration of the image segmentation and texture feature extraction at different spatial frequencies is outlined in Fig. 1. Following the filtration step, quantification of texture using statistical and histogram characteristics comprised of mean intensity, standard deviation (SD), entropy, mean of positive pixels (MPP), skewness and kurtosis. Mean intensity describes the average intensity value of pixels in a defined region of interest. SD reflects variation/deviation of the pixel values about the mean. Entropy is a statistical parameter which measures irregularity; the higher the value the more irregular is the texture. In addition to the mean intensity, MPP measures the average intensity of the pixels with only positive values. Skewness reflects an asymmetry in the histogram distribution about the mean. Kurtosis indicates how peaked/pointed the histogram is relative to a normal distribution. An illustration of the quantification process using histogram-based statistical analysis is in Fig. 2. Miles et al. [17] have described in detail what filtration-histogram based TA mean and how the texture features reflect different components of heterogeneity (object size, number of objects and variation in the intensity of the objects in relation to the background).

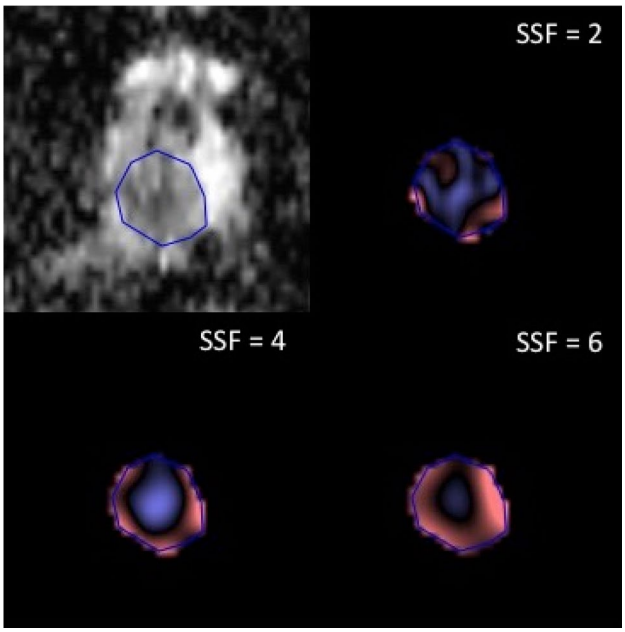

Fig. 1 Segmented ADC map of high-grade Gleason 4+5 MR-visible tumour focus with fine (SSF=2), medium (SSF=4) and coarse (SSF=6) spatial features extracted prior to texture analysis

Unlike ADC, absolute *T*2 weighted and post-contrast weighted pixel values are not normalized. Consequently, texture features that are calculated from absolute *T*2 and post-contrast pixel values such as the mean, SD, MPP were excluded from the analysis of *T*2 and post-contrast *T*1. Texture features that are calculated from the shape of the *T*2 or post-contrast histogram (such as entropy, skewness, kurtosis) are not affected by the absolute pixel value and were included.

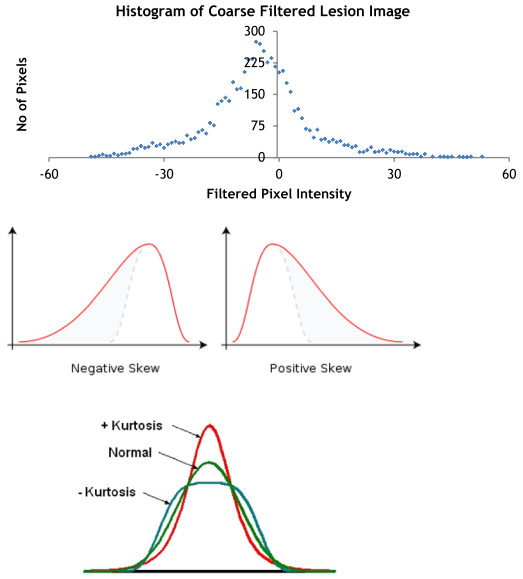

Fig. 2 Illustration of texture quantification using a histogram-based statistical analysis. Mean: The average value of the pixels within the region of interest. Standard deviation—a measure of how much variation or "dispersion" exists from the average. Skewness—symmetry of the distribution may reflect structures (bright or dark objects). Kurtosis—pointiness of the distribution may reflect increased contrast. Entropy—measures irregularity or complexity, indicated by a higher value

Statistical analysis

We used the non-parametric Spearman's rank correlation to assess the primary endpoint of the association between MRTA parameters and GS. Additionally, we assessed the correlation with the D'Amico score and PSA as secondary outcome measures. We used SPSS statistics for Windows for statistical analysis (version 25; IBM, Armonk, NY, USA) and p value < 0.05 was considered as significant.

Results

Of the 26 men included, tumours were visible on ADC in 25, Contrast in 26 and *T*2 in 24 cases. Therefore, the details of these 26 patients were used for the purpose of the study. The demographic details of these patients along with their GS, D'Amico risk and PSA are in Table 1.

MR ADC texture parameters showed a significant, negative correlation with Gleason score particularly at medium texture scale SSF = 5 (MPP rs = − 0.493, $p = 0.009$, SD rs = − 0.382, $p = 0.049$) and coarse texture scale SSF = 6 (MPP rs = − 0.490, $p = 0.009$, SD rs = − 0.485, $p = 0.010$). ADC mean demonstrated a negative correlation with Gleason score (rs = − 0.402, $p = 0.038$). MR Contrast texture without filtration showed a significant, negative correlation with D'Amico risk (skewness rs = − 0.492, $p = 0.006$). MR *T*2 texture parameters showed a significant, negative correlation with D'Amico at texture without filtration (Skewness rs = − 0.455, $p = 0.019$), medium texture scales (Skewness rs = − 0.399, $p = 0.043$) and coarse texture scales (Skewness rs = − 0.400, $p = 0.043$, Kurtosis rs = − 0.424, $p = 0.031$). A summary of significant results is detailed in Table 4. No significant correlation was obtained between MRTA parameters and serum PSA in our cohort.

In summary, ADC parameters negatively correlated with Gleason score, whereas *T*2 and post-contrast texture features negatively correlated with D'Amico score.

Discussion

We studied the ability of mpMRI derived TA to predict the Gleason Score, D'Amico risk and explored the association between texture analysis and total PSA in a cohort of prostate cancer patients who underwent prostatectomy. In most cases, we were able to accurately correlate the tumour focus

Table 4 Results summary of statistically significant correlations between ADC, contrast enhancement and *T*2 texture analysis with both Gleason grade and D'Amico score, *SD* standard deviation, *MPP* mean of positive pixels

Sequence	Statistical test	Filter	Outcome	Feature	Correlation (rs)	P-value
ADC	Spearman	0	Gleason	Mean	− 0.402	0.038
ADC	Spearman	4	Gleason	Mean	− 0.404	0.037
ADC	Spearman	5	Gleason	mpp	− 0.493	0.009
ADC	Spearman	5	Gleason	sd	− 0.382	0.049
ADC	Spearman	6	Gleason	mpp	− 0.49	0.009
ADC	Spearman	6	Gleason	sd	− 0.485	0.01
ADC	KW	6	Gleason	Skewness		0.028
Contrast	Spearman	0	D'Amico	Skewness	− 0.492	0.006
Contrast	KW	0	D'Amico	Skewness		0.029
*T*2	Spearman	0	D'Amico	Skewness	− 0.455	0.019
*T*2	Spearman	5	D'Amico	Skewness	− 0.399	0.043
*T*2	Spearman	6	D'Amico	Skewness	− 0.400	0.043
*T*2	Spearman	6	D'Amico	Kurtosis	− 0.424	0.031

from the histopathological specimen rather than inferring this from a representative biopsy.

We found that ADC texture parameters negatively correlated with GS, whereas *T*2 and post-contrast texture features negatively correlated with the D'Amico score.

mpMRI has transformed oncological imaging and has been harnessed for tumour grading and detection, as well as for prognostication and monitor response to treatment. MRTA is emerging as a potential tool in prostate cancer imaging and may help to prevent over-treatment of clinically insignificant tumours. This is mainly an issue with anteriorly located tumours [24]. mpMRI can differentiate central gland tumour from benign hyperplasia, a traditionally difficult area to evaluate with traditional MR imaging [25].

Our findings suggest that specific textural features aid classification of GS. We found that the mean, mean of positive pixels (MPP), and SD have a significant negative correlation with GS on ADC. Interestingly, fine texture scales were not predictive whereas techniques without filtration or with high end texture scales did have correlations. We hypothesise that fine texture scale (2 mm) features may not be reflective of biologically important features as at that scale heterogeneity assessment via texture analysis may be more prone to variation in image acquisition parameters.

We chose to also include correlation with the D'Amico score as an outcome measure. This tool calculates the 5-year risk of treatment failure based upon the serum PSA, Gleason grade and clinical stage, thus integrating clinical data with histology and radiology [1]. The score includes a GS of ≤ 6 as part of the low-risk stratification criteria (Table 1). Our rationale was to attempt to address some of the limitations in defining 'clinically significant' disease based on the GS alone. The majority of prior work in the literature regarding texture analysis has focused only on the traditional GS in patient risk stratification [23, 26, 28].

We found that skewness showed a significant negative correlation with the D'Amico score on post-contrast MRTA without filtration. On *T*2-weighted sequences, skewness and kurtosis demonstrated a significant negative correlation with the D'Amico score at medium and coarse texture scales, particularly at texture without filtration. There was no significant correlation with GS alone for the texture parameters on *T*2-weighted or contrast-enhanced sequences.

We could not demonstrate any correlation between texture parameters and the serum PSA alone in our cohort. This absence of correlation with the serum total PSA is not surprising, given the high level of false-positive results of this test when used alone [29].

Our findings suggest that high-grade prostate malignancies, i.e., with adverse tumour biology, are more heterogeneous than low grade, clinically insignificant tumours. Increased tumour heterogeneity has been previously linked to worse clinical prognosis in multiple tumour types, including oesophageal, colorectal, CNS, and non-small cell lung carcinoma. Furthermore, texture analysis can provide prognostic information from imaging, additional to that given by a radiologist, and be useful as an independent predictor of survival [19, 30]. Texture analysis has also been harnessed in breast, rectal, renal cell, and pancreatic cancer as an early indicator of treatment response [10–15, 30].

Our study corroborates previous work by Dikaios et al. who used logistic regression models based upon quantitative mpMRI parameters, such as ADC, in 155 patients to differentiate between benign (GS six or less) and malignant lesions in the transition zone (TZ) [23]. This has also been demonstrated in a cohort of patients with peripheral zone tumours [24]. Wibmer et al. showed that peripheral zone tumours had significantly lower homogeneity on ADC maps and *T*2-weighted imaging compared to benign tissue in a cohort of 147 patients [26].

Regarding particular texture parameters, our results are supported by a previous study where there was reduced mean intensity, MPP and SD in TZ tumours [27]. In particular, these findings were present in TZ tumours with adverse biology as indicated by abnormal PSA expression on corresponding PET images. This indication of abnormal tumour biology by the mean, MPP and SD is likewise suggested by our findings of a negative correlation with a high GS or the D'Amico risk stratification. The lower mean and MPP post-filtration of high-grade malignancy is in keeping with clinically significant tumours with high cellularity generally having low ADC values. This implies a translational benefit where these MRI parameters on texture analysis might better) inform clinicians about the risks of high-grade disease through a non-invasive method than merely measuring the ADC mean which was less significant in our study.

A less peaked distribution (i.e., more plateaued distribution) may reflect lower tissue contrast and more cellularity or lower kurtosis and lower/negative skewness (i.e., preponderance of darker features and more cellularity) of pixel signal intensity on *T*2-weighted sequences, predicted high-grade tumours in our study. Sidhu et al. used a cohort of 26 patients to demonstrate that MRTA of TZ tumours can discriminate significant prostate cancer, as deemed by template-mapping biopsy and GS [28]. A reduced ADC kurtosis, reflecting less peaked histogram distribution of pixel values, was found to be the best textural parameter for classifying significant TZ tumours. Furthermore, in a cohort of 180 endometrial cancer patients, kurtosis on contrast-enhanced images negatively predicted recurrence and progression-free survival [19].

Other groups have noted the significance of skewness in determining high-grade cancer [20]. It has been proposed that histograms are less skewed in malignant tumours with high cellularity due to the densely packed cells [18].

There are a few limitations to our study. Firstly, the sample size was small, as we only included patients who

had MRI-visible tumours. Secondly, we used 1.5T scanners exclusively in our cohort. Applicability of our findings to a higher Tesla scanner has not formally been assessed, although guidance from a European Consensus meeting advocates a 1.5T mpMRI protocol [31]. The use of endorectal coils was not deemed necessary by this group, and accordingly, we did not use such coils. Studies have found an equivocal performance of mpMRI at 1.5T using endorectal coils, compared to imaging without endorectal coils [31–34]. A potential source of error may have been introduced during manual contouring of region of interests. We envisage that future use of machine learning with automated segmentation would negate this issue. There is much variability in prostate tumour cellularity which is not factored into the current Gleason grading system [35]. Hence, there are limitations of the Gleason score to determine significant high-grade tumours. Indeed, sparse prostate tumours can have equivalent ADC and *T*2 pixel values to normal prostatic tissue [35]. We have partially addressed this issue by including a correlation with the D'Amico classification system. Our study population only includes patients who underwent prostatectomy so there may have been a selection bias towards more aggressive tumours potentially missing lower grade cancers that may ultimately benefit from non-invasive assessment. As the purpose of our study was to examine for the applicability of MR texture analysis technology to assess if filtration-histogram analysis helps in defining clinically significant cancer, we did not study if the tumour arose from the peripheral zone or transition zone.

Our study has some strengths as well. An important distinguishing feature of our study is the use of whole gland prostatectomy specimens for histology. We had access to histopathology data which enabled a precise pathological correlate to mpMRI imaging features, rather than inferring this from a representative biopsy. For the same reason, we had only selected patients with visible tumour foci, enabling an accurate co-relation with the tumour. Furthermore, to our knowledge, this is the only study to use variables other than GS alone to determine 'clinically significant' tumours as we used the D'Amico score and serum PSA as well. The D'Amico classification is a clinical score that uses the whole gland and not just the ROI and, hence, may not be expected to correlate with TA. Therefore, our observations linking TA with a well-validated prognostic scale such as the D'Amico adds strength to the value of our study.

In summary, MRTA may be used as a non-invasive imaging biomarker to guide risk stratification, prognosis, treatment, and follow-up. This preliminary study suggests that medium texture scale (3–5 mm features) may better reflect biological heterogeneity and may be more useful.

Thus, MRTA can guide personalised decision making, including prevention of over-diagnosis and over-treatment of clinically insignificant disease. One potential future application of the work is in the group of patients with occult tumours which are not visible with conventional MRI yet malignancy is indicated on histology. Another potential application is for non-invasive follow-up of less aggressive tumours or those on active surveillance, perhaps avoiding sequential biopsies. Currently, there are only a small number of clinical studies on MRTA and its correlation to clinically relevant prognostic markers. Our findings would need validation in further studies.

When used as a multi-parametric computer-aided detection (CAD) model, an objective textural assessment could improve prostate cancer classification, especially in cases where radiologists are uncertain. In the United Kingdom, the use of mpMRI in prostate cancer patients with a negative non-targeted TRUS biopsy has already been advocated by NICE [4]. The application of MR texture analysis to this cohort should lead to a more appropriate selection of patients to individual treatment pathways.

Author contributions AA: study conceptualisation. BG: MR image analysis (guidance), statistics and inputs to the manuscript. DB: Study conceptualisation, clinical data collection, manuscript revisions. JS: MR image analysis and manuscript revisions. MH: Initial draft, bibliography and manuscript revisions. SM: Clinical data collection and validation. Control of data and final manuscript approval were undertaken by the last author (study-guarantor).

Funding BG and AA work at University College London Hospital/University College London (UCLH/UCL), which received a proportion of the funding from the UK's Department of Health's National Institute of Health Research, Biomedical Research Centre's funding scheme. AA has also received funding from the London North West Healthcare Charitable Fund and the UCL Experimental Cancer Medicine Centre.

Compliance with ethical standards

Conflict of interest BG is a Director of Feedback Medical Ltd (www.fbkmed.com) and Shareholder of Feedback Plc, Cambridge (which wholly owns Feedback Medical Ltd.), a UK-based medical imaging software company and manufacturer of TexRAD texture analysis research software used in this study.

Ethical approval All procedures performed in studies involving human participants were in accordance with the ethical standards of the institutional and/or national research committee and with the 1964 Helsinki declaration and its later amendments or comparable ethical standards. This article does not contain any studies with animals performed by any of the authors.

References

1. D'Amico A (1998) Biochemical outcome after radical prostatectomy, external beam radiation therapy, or interstitial radiation therapy for clinically localized prostate cancer. JAMA 280(11):969
2. Klotz L, Zhang L, Lam A, Nam R, Mamedov A, Loblaw A (2010) Clinical results of long-term follow-up of a large, active

surveillance cohort with localized prostate cancer. J Clin Oncol 28:126–131
3. Heidenreich A, Bastian PJ, Bellmunt J et al (2014) EAU guidelines on prostate cancer. Part 1: screening, diagnosis, and local treatment with curative intent-update 2013. Eur Urol 65:124–137. https://doi.org/10.1016/j.eururo.2013.1009.1046 (**Epub 2013 Oct 1016**)
4. Nice.org.uk. (2018). Prostate cancer: diagnosis and management |Guidance and guidelines| NICE. http://www.nice.org.uk/guidance/cg175. Accessed 28 May 2018
5. Delongchamps N, Rouanne M, Flam T, Beuvon F, Liberatore M, Zerbib M, Cornud F (2011) Multiparametric magnetic resonance imaging for the detection and localization of prostate cancer: combination of *T*2-weighted, dynamic contrast-enhanced and diffusion-weighted imaging. BJU Int 107(9):1411–1418
6. Berglund R, Masterson T, Vora K, Eggener S, Eastham J, Guillonneau B (2008) Pathological upgrading and up staging with immediate repeat biopsy in patients eligible for active surveillance. J Urol 180(5):1964–1968
7. Kasivisvanathan V, Rannikko AS, Borghi M, Panebianco V, Mynderse LA, Vaarala MH et al (2018) MRI-targeted or standard biopsy for prostate-cancer diagnosis. N Engl J Med 378(19):1767–1777
8. Sahibzada I, Batura D, Hellawell G (2016) Validating multiparametric MRI for diagnosis and monitoring of prostate cancer in patients for active surveillance. Int Urol Nephrol 48(4):529–533
9. Barentsz J, Richenberg J, Clements R, Choyke P, Verma S, Villeirs G, Rouviere O, Logager V, Fütterer J (2012) ESUR prostate MR guidelines 2012. Eur Radiol 22(4):746–757
10. Eliat P, Olivié D, Saïkali S, Carsin B, Saint-Jalmes H, de Certaines J (2012) Can dynamic contrast-enhanced magnetic resonance imaging combined with texture analysis differentiate malignant glioneuronal tumors from other glioblastoma? Neurol Res Int 2012:1–7
11. Parikh J, Selmi M, Charles-Edwards G, Glendenning J, Ganeshan B, Verma H, Mansi J, Harries M, Tutt A, Goh V (2014) Changes in primary breast cancer heterogeneity may augment midtreatment MR imaging assessment of response to neoadjuvant chemotherapy. Radiology 272(1):100–112
12. De Cecco C, Ganeshan B, Ciolina M, Rengo M, Meinel F, Musio D, De Felice F, Raffetto N, Tombolini V, Laghi A (2015) Texture analysis as imaging biomarker of tumoral response to neoadjuvant chemoradiotherapy in rectal cancer patients studied with 3-t magnetic resonance. Invest Radiol 50(4):239–245
13. Ganeshan B, Panayiotou E, Burnand K, Dizdarevic S, Miles K (2011) Tumour heterogeneity in non-small cell lung carcinoma assessed by CT texture analysis: a potential marker of survival. Eur Radiol 22(4):796–802
14. Miles K, Ganeshan B, Griffiths M, Young R, Chatwin C (2009) Colorectal cancer: texture analysis of portal phase hepatic CT images as a potential marker of survival. Radiology 250(2):444–452
15. Ganeshan B, Skogen K, Pressney I, Coutroubis D, Miles K (2012) Tumour heterogeneity in oesophageal cancer assessed by CT texture analysis: preliminary evidence of an association with tumour metabolism, stage, and survival. Clin Radiol 67(2):157–164
16. Davnall F, Yip C, Ljungqvist G, Selmi M, Ng F, Sanghera B, Ganeshan B, Miles K, Cook G, Goh V (2012) Assessment of tumor heterogeneity: an emerging imaging tool for clinical practice? Insights Imaging 3(6):573–589
17. Miles K, Ganeshan B, Hayball M (2013) CT texture analysis using the filtration-histogram method: what do the measurements mean? Cancer Imaging 13(3):400–406
18. Donati O, Mazaheri Y, Afaq A, Vargas H, Zheng J, Moskowitz C, Hricak H, Akin O (2014) Prostate cancer aggressiveness: assessment with whole-lesion histogram analysis of the apparent diffusion coefficient. Radiology 271(1):143–152
19. Ytre-Hauge S, Dybvik J, Lundervold A, Salvesen Ø, Krakstad C, Fasmer K, Werner H, Ganeshan B, Høivik E, Bjørge L, Trovik J, Haldorsen I (2018) Preoperative tumor texture analysis on MRI predicts high-risk disease and reduced survival in endometrial cancer. J Magn Reson Imaging 48(6):1637–1647
20. Schob S, Meyer H, Dieckow J, Pervinder B, Pazaitis N, Höhn A, Garnov N, Horvath-Rizea D, Hoffmann K, Surov A (2017) Histogram analysis of diffusion weighted imaging at 3T is useful for prediction of lymphatic metastatic spread, proliferative activity, and cellularity in thyroid cancer. Int J Mol Sci 18(4):821
21. Health Research Authority. (2019). Homepage. https://www.hra.nhs.uk/. Accessed 3 Feb 2019
22. Pierorazio P, Walsh P, Partin A, Epstein J (2013) Prognostic Gleason grade grouping: data based on the modified Gleason scoring system. BJU Int 111(5):753–760
23. Dikaios N, Alkalbani J, Sidhu H, Fujiwara T, Abd-Alazeez M, Kirkham A, Allen C, Ahmed H, Emberton M, Freeman A, Halligan S, Taylor S, Atkinson D, Punwani S (2014) Logistic regression model for diagnosis of transition zone prostate cancer on multi-parametric MRI. Eur Radiol 25(2):523–532
24. Langer D, van der Kwast T, Evans A, Trachtenberg J, Wilson B, Haider M (2009) Prostate cancer detection with multi-parametric MRI: logistic regression analysis of quantitative *T*2, diffusion-weighted imaging, and dynamic contrast-enhanced MRI. J Magn Reson Imaging 30(2):327–334
25. Oto A, Kayhan A, Jiang Y, Tretiakova M, Yang C, Antic T, Dahi F, Shalhav A, Karczmar G, Stadler W (2010) Prostate cancer: differentiation of central gland cancer from benign prostatic hyperplasia by using diffusion-weighted and dynamic contrast-enhanced MR imaging. Radiology 257(3):715–723
26. Wibmer A, Hricak H, Gondo T, Matsumoto K, Veeraraghavan H, Fehr D, Zheng J, Goldman D, Moskowitz C, Fine S, Reuter V, Eastham J, Sala E, Vargas H (2015) Haralick texture analysis of prostate MRI: utility for differentiating non-cancerous prostate from prostate cancer and differentiating prostate cancers with different Gleason scores. Eur Radiol 25(10):2840–2850
27. Bates A, Miles K (2017) Prostate-specific membrane antigen PET/MRI validation of MR textural analysis for detection of transition zone prostate cancer. Eur Radiol 27(12):5290–5298
28. Sidhu H, Benigno S, Ganeshan B, Dikaios N, Johnston E, Allen C, Kirkham A, Groves A, Ahmed H, Emberton M, Taylor S, Halligan S, Punwani S (2016) Textural analysis of multiparametric MRI detects transition zone prostate cancer. Eur Radiol 27(6):2348–2358
29. Barry MJ (2001) Clinical practice prostate-specific-antigen testing for early diagnosis of prostate cancer. N Engl J Med 344(18):1373–1377
30. Yoon H-J, Kim Y, Chung J, Kim BS (2018) Predicting neoadjuvant chemotherapy response and progression-free survival of locally advanced breast cancer using textural features of intratumoral heterogeneity on F-18 FDG PET/CT and diffusion-weighted MR imaging. Breast J. https://doi.org/10.1111/tbj.13032
31. Dickinson L, Ahmed H, Allen C, Barentsz J, Carey B, Futterer J, Heijmink S, Hoskin P, Kirkham A, Padhani A, Persad R, Puech P, Punwani S, Sohaib A, Tombal B, Villers A, van der Meulen J, Emberton M (2011) Magnetic resonance imaging for the detection, localisation, and characterisation of prostate cancer: recommendations from a European consensus meeting. Eur Urol 59(4):477–494
32. Taira A, Merrick G, Galbreath R, Andreini H, Taubenslag W, Curtis R, Butler W, Adamovich E, Wallner K (2009) Performance of transperineal template-guided mapping biopsy in detecting prostate cancer in the initial and repeat biopsy setting. Prostate Cancer Prostatic Dis 13(1):71–77

33. Bratan F, Niaf E, Melodelima C, Chesnais A, Souchon R, Mège-Lechevallier F, Colombel M, Rouvière O (2013) Influence of imaging and histological factors on prostate cancer detection and localisation on multiparametric MRI: a prospective study. Eur Radiol 23(7):2019–2029
34. Lee S, Park K, Choi K, Lim B, Kim J, Lee S, Chung B (2010) Is endorectal coil necessary for the staging of clinically localized prostate cancer? Comparison of non-endorectal versus endorectal MR imaging. World J Urol 28(6):667–672
35. Langer D, van der Kwast T, Evans A, Sun L, Yaffe M, Trachtenberg J, Haider M (2008) Intermixed normal tissue within prostate cancer: effect on MR imaging measurements of apparent diffusion coefficient and *T*2—sparse versus dense cancers. Radiology 249(3):900–908

Publisher's Note Springer Nature remains neutral with regard to jurisdictional claims in published maps and institutional affiliations.